International Journal of Basic & Clinical Pharmacology
Rymbai M et al. Int J Basic Clin Pharmacol. 2026 Nov;15(6):1144-1152
https://www.ijbcp.com
pISSN 2319-2003 | eISSN 2279-0780

DOI: https://dx.doi.org/10.18203/2319-2003.ijbcp20263255

Original Research Article

Phenotypic adaptation of clinical *Pseudomonas aeruginosa* to increasing ceftazidime exposure

Maxmillando Rymbai*, Vedant V. Borah

Department of Bio-Sciences, School of Life Sciences, Assam Don Bosco University, Tapesia, Sonapur, Assam, India

Received: 28 July 2026
Accepted: 31 August 2026

***Correspondence:**
Maxmillando Rymbai,
Email: maxmillandorymbai@gmail.com

Copyright: © the author(s), publisher and licensee Medip Academy. This is an open-access article distributed under the terms of the Creative Commons Attribution Non-Commercial License, which permits unrestricted non-commercial use, distribution, and reproduction in any medium, provided the original work is properly cited.

ABSTRACT

Background: *Pseudomonas aeruginosa* readily adapts to antibiotic stress, but the effect of increasing ceftazidime exposure on colony morphology across specimen sources is poorly defined. This study determined whether ceftazidime alters growth and colony morphology in a concentration-dependent manner and whether the response varies by specimen source.
Methods: Forty-eight non-duplicate clinical *P. aeruginosa* isolates from pus, wound swabs, urine, and tracheal aspirates were characterised for ceftazidime susceptibility, extended-spectrum β-lactamase (ESBL) and metallo-β-lactamase (MBL) production, and biofilm formation. Colony morphology was assessed after 24 hours on M9 agar with Congo red and Coomassie brilliant blue (RB medium), alone and with ceftazidime at one-half, one, and two times the isolate-specific minimum inhibitory concentration (MIC).
Results: Ceftazidime resistance was 70.8%, ESBL production 47.9%, MBL production 33.3%, and strong biofilm formation 45.8%. Growth fell from 97.9% on RB medium to 45.8% at twice the MIC ($p<0.001$). Mean colony diameter decreased from 19.59 to 5.00 mm among growing isolates, and from 19.18 to 2.29 mm when non-viable colonies were scored as 0 mm ($p<0.001$). Colony diameter differed by specimen source under every condition ($p<0.05$); tracheal aspirate isolates retained the largest median diameter at and above the MIC. Morphology was characterised by small, round, flat, dry, red colonies.
Conclusions: Ceftazidime produced dose-dependent reductions in bacterial growth and colony morphological variety, indicating phenotypic adaptation not detected by routine susceptibility testing. The response differed by specimen source, with respiratory isolates retaining the greatest growth capacity under drug pressure.

Keywords: *Pseudomonas aeruginosa*, Ceftazidime, Colony morphology, Antimicrobial resistance, Biofilm, Congo red

INTRODUCTION

Pseudomonas aeruginosa is an opportunistic gram-negative bacterium that is a leading cause of healthcare-associated infections worldwide. It is frequently associated with respiratory tract infections, wound and burn infections, urinary tract infections, bloodstream infections, and infections among immunocompromised and critically ill patients.[1,2] The remarkable adaptability of *P. aeruginosa* enables it to survive in diverse environmental niches and hospital settings, contributing to persistent infections and increased healthcare burden.[3] The organism possesses numerous virulence determinants, including quorum sensing systems, extracellular enzymes, toxins, and biofilm-forming ability, which collectively enhance colonisation, persistence, and pathogenicity.[4,5]

Managing *P. aeruginosa* infections is difficult because the organism combines intrinsic resistance with a capacity to take up further resistance determinants.[6,7] Ceftazidime, a third-generation antipseudomonal cephalosporin, is among the β-lactams commonly used against *P. aeruginosa* infections.[8] Sustained antibiotic exposure has, however, selected for resistant strains that draw on several mechanisms at once: extended-spectrum β-lactamases (ESBLs) and metallo-β-lactamases (MBLs), together with

reduced outer membrane permeability, active efflux, and target-site changes.[9,10] These mechanisms often occur together, producing multidrug-resistant isolates that leave few treatment options and worsen clinical outcomes.[11,12]

Biofilm formation is another adaptive strategy of *P. aeruginosa*. Cells within a biofilm sit inside a self-produced extracellular matrix that shields them from antimicrobials, host defences, and environmental stress.[13,14] As a result, biofilm-grown isolates tend to persist longer and tolerate antibiotics better than their planktonic counterparts.[15,16] Because resistance and biofilm formation together drive chronic and recurrent infection, their interaction has been studied extensively.[17]

In addition to these well-recognised resistance mechanisms, *P. aeruginosa* shows marked phenotypic plasticity in response to environmental and antimicrobial stress. Changes in colony morphology represent visible manifestations of bacterial adaptation and may reflect alterations in extracellular matrix production, cellular physiology, metabolic activity, and stress-response pathways.[18,19] Colony characteristics such as diameter, colour, surface texture, form, elevation, and margin have long been recognised as useful phenotypic indicators in microbiological investigations.[20] Media supplemented with Congo red and Coomassie brilliant blue facilitate visualisation of colony architecture and extracellular matrix-associated phenotypes, thereby providing an effective platform for investigating adaptive morphological responses.[21,22]

Although numerous studies have investigated antimicrobial susceptibility, β-lactamase production, and biofilm formation in clinical *P. aeruginosa* isolates, comparatively few have examined the influence of increasing concentrations of ceftazidime on colony morphology under controlled experimental conditions.[23] Furthermore, limited information is available regarding the morphological adaptation of clinical isolates from different specimen sources when cultured on M9 minimal agar supplemented with Congo red and Coomassie brilliant blue. Characterising these phenotypic responses may improve our understanding of bacterial adaptation to antibiotic stress and provide additional insight into the relationship between antimicrobial exposure, colony architecture, and bacterial persistence.[24]

Therefore, the present study investigated the colony morphology changes in representative clinical *P. aeruginosa* isolates recovered from pus, wound swabs, urine, and tracheal aspirate specimens under increasing concentrations of ceftazidime. Isolates were selected based on three criteria: ceftazidime susceptibility determined by VITEK 2 compact, β-lactamase production confirmed phenotypically, and biofilm-forming ability measured by crystal violet assay. Colony morphology was evaluated on M9 minimal agar supplemented with Congo red and Coomassie brilliant blue. Morphological characteristics, including colony growth, diameter, form, colour, surface texture, elevation, and margin, were systematically assessed to determine phenotypic adaptation under antibiotic stress.

METHODS

Bacterial isolates

The overall experimental workflow is shown in Figure 1. A total of 48 non-duplicate clinical *P. aeruginosa* isolates, each recovered from a separate patient, were obtained from the department of microbiology, Nazareth Hospital. Each isolate was characterized phenotypically. The isolates were recovered from routine clinical specimens, including pus, wound swabs, urine, and tracheal aspirates, and were identified using the VITEK 2 Compact system (bioMérieux, France).[25] Confirmed isolates were transferred to the department of microbiology, Assam Don Bosco University, where they were sub-cultured on nutrient agar and incubated at 37°C for 18-24 hours before further analysis (Figure 1).

Phenotypic characterization

Phenotypic characterization was performed using CLSI M100 (2026) guidelines, and the results were used to select representative isolates for the colony morphology study.[26] Ceftazidime susceptibility was determined using the Kirby-Bauer disk diffusion method with a 30-µg ceftazidime disk.[27] ESBL production was detected using the combined disk method with ceftazidime and ceftazidime-clavulanic acid disks.[28] MBL production was detected using the imipenem-EDTA combined disk method.[29] Ceftazidime-susceptible isolates were defined based on VITEK 2 compact minimum inhibitory concentration results interpreted according to CLSI M100 (2026) breakpoints.

Biofilm formation was assessed using a crystal violet microtitre plate assay. Isolates were grown in tryptic soy broth (TSB) in sterile 96-well polystyrene microtitre plates at 37°C for 24 hours. Following PBS washing, adherent biofilms were stained with 0.1% crystal violet, destained with 30% acetic acid, and the optical density was measured at 570 nm. Biofilm-forming ability was categorised using the optical density cut-off (ODc) method as non, weak, moderate, or strong.[30]

Selection of representative isolates

Forty-eight representative *P. aeruginosa* isolates were selected from four specimen sources (pus, wound swabs, urine, and tracheal aspirates). The selected isolates represented clinically relevant phenotypic categories: ESBL producers and MBL producers, defined by combined disk testing; strong biofilm-forming isolates, defined by the crystal violet microtitre assay; and ceftazidime-susceptible isolates, defined by VITEK 2 compact susceptibility results. On each plate, four representative isolates were arranged at fixed positions:

position 1, an ESBL producer; position 2, an MBL producer; position 3, a strong biofilm former; and position 4, a ceftazidime-susceptible isolate. Because these categories are not mutually exclusive (a single isolate may, for example, be both an ESBL and an MBL producer as well as a strong biofilm former), each isolate was assigned to one primary category for the purpose of plate position only, whereas the group frequencies reported in Table 1 reflect all categories to which an isolate belonged.

Colony morphology assay

Colony morphology was evaluated on M9 minimal agar prepared from HiMedia M9 minimal salt (1×) powder (1.12 g/100 ml) supplemented with agar (15 g/l) (HiMedia). Congo red was added at a final concentration of 50 mg/l, followed by Coomassie brilliant blue G-250 (10 mg/l). Analytical-grade ceftazidime pentahydrate powder (HiMedia Laboratories Pvt. Ltd., India; product code: CMS1194) was dissolved in sterile distilled water and incorporated into molten agar after cooling to approximately 50°C. The concentration of ceftazidime was determined according to the isolate-specific minimum inhibitory concentration (MIC) previously established using the VITEK 2 compact system. Five experimental conditions were evaluated: M9 control, RB medium (M9 supplemented with Congo red and Coomassie brilliant blue), and RB medium supplemented with ceftazidime at one-half of the isolate-specific minimum inhibitory concentration (MIC) (½× MIC), isolate-specific MIC (1× MIC), and twice the isolate-specific MIC (2× MIC).

For each specimen source, four representative isolates were inoculated onto a single agar plate at predetermined locations on the plate. Each condition was set up on three independently prepared replicate plates carrying the same four isolates. The plates were incubated aerobically at 37°C for 24 hours. Each colony was scored for growth, diameter, form, colour, surface, elevation, and margin. Diameters were measured in millimetres using a HiMedia colony measuring scale, and morphological descriptors followed standard microbiological criteria.

Statistical analysis

Data were analysed using IBM statistical package for the social sciences (SPSS) statistics version 20.0. Categorical variables are presented as frequencies and percentages, and colony diameter as mean ± standard deviation. The diameter was handled in two ways, as neither approach alone fully describes the response. The first counts only isolate that grew under a given condition and separates the effect on colony size from the effect on viability. The second method counts all 48 isolates and scores a non-viable colony as 0 mm, combining growth inhibition and size reduction in a single measure. Both are reported. Because the same isolates were assessed under all five conditions, every comparison across conditions used a test for related samples; the Kruskal-Wallis and Chi-square tests assume independent groups and do not suit this study design. The diameter across conditions was compared using the Friedman test, with Wilcoxon signed-rank post-hoc tests and Bonferroni correction. The proportion of growing isolates was compared using Cochran's Q test, with pairwise McNemar tests and Bonferroni correction. The diameter was also compared between specimen sources (mutually exclusive groups of equal size [n=12 each]) using the Kruskal-Walli's test. Significance was set at $p<0.05$.

RESULTS

Characteristics of the representative clinical P. aeruginosa isolates

A total of 48 representatives clinical *P. aeruginosa* isolates, comprising 12 isolates each from pus, wound swabs, urine, and tracheal aspirate specimens, were included in the study (Table 1). Overall, 34 (70.8%) isolates were resistant to ceftazidime, and 23 (47.9%) and 16 (33.3%) were positive for ESBL and MBL production, respectively. Tracheal aspirate isolates showed the highest proportion of ceftazidime resistance (83.3%) and ESBL production (58.3%) among the isolates. Strong biofilm formation was observed in 22 (45.8%) isolates, with wound swab isolates demonstrating the highest proportion (83.3%) (Table 1).

Effect of increasing ceftazidime concentrations on colony growth and colony diameter

The effect of increasing ceftazidime concentrations on bacterial growth and colony diameter is summarised in Table 2 and illustrated in Figure 2. Comparable bacterial growth was observed on M9 control and RB agars, with 46 (95.8%) and 47 (97.9%) isolates exhibiting visible growth, respectively. However, growth progressively declined following ceftazidime supplementation, decreasing to 31 (64.6%) isolates at ½× MIC, 24 (50.0%) at 1× MIC, and 22 (45.8%) at 2× MIC. The difference in the proportion of isolates showing visible growth across the five conditions was statistically significant (Cochran's $Q=75.47$, $df=4$, $p<0.001$), and pairwise McNemar tests confirmed a significant loss of growth relative to the RB medium at each ceftazidime concentration (all adjusted $p<0.001$). Correspondingly, the proportion of isolates showing no visible growth increased from 2.1% on RB medium to 35.4% at ½× MIC, 50.0% at 1× MIC, and 54.2% at 2× MIC.

A similar trend was observed for the colony diameter. Among isolates showing visible growth, the mean colony diameter was 20.57±16.91 mm on M9 agar and 19.59±9.48 mm on RB agar, falling to 6.13±1.67 mm, 5.83±1.74 mm, and 5.00±1.45 mm at ½×MIC, 1×MIC, and 2×MIC, respectively. When all 48 isolates were included and non-viable colonies were assigned 0 mm, the corresponding values were 19.71±17.06 mm, 19.18±9.79 mm, 3.96±3.25 mm, 2.92±3.19 mm, and 2.29±2.70 mm. The larger reduction in the second analysis reflected the

additional contribution of complete growth inhibition. Notably, in the all-isolate analysis, the standard deviation exceeded the mean at 1× and 2× MIC, a consequence of the high proportion of zero values (50.0% and 54.2%, respectively); the median colony diameter was 2.00 mm (IQR 0.00-6.00) at 1× MIC and 0.00 mm (IQR 0.00-5.00) at 2× MIC. The reduction in colony diameter across the five conditions was statistically significant (Friedman test: χ^2=149.00, df=4, p<0.001). Post-hoc Wilcoxon signed-rank tests with Bonferroni correction confirmed that colony diameter was significantly lower than on RB medium at ½× MIC, 1× MIC, and 2× MIC (all adjusted P <0.001), and that each successive increase in ceftazidime concentration produced a further significant reduction (½× versus 1× MIC, adjusted p=0.037; 1× versus 2× MIC, adjusted p=0.011; ½× versus 2× MIC, adjusted p<0.001). Colony diameter did not differ significantly between the M9 and RB media (adjusted p=1.000), indicating that the RB medium itself did not inhibit growth (Table 2 and Figure 2).

Effect of increasing ceftazidime concentrations on colony morphology

The predominant colony morphologies observed under each experimental condition are presented in Table 3, with representative photographs of the colonies shown in Figure 3. Colonies grown on M9 control agar exhibited diverse morphologies, including round, irregular, and wrinkled forms with predominantly white pigmentation and dry, shiny, or mucoid surfaces. Similar morphological characteristics were observed on RB agar, although colony pigmentation and surface features were more clearly visualised. Exposure to increasing isolate-specific concentrations of analytical-grade ceftazidime pentahydrate resulted in a progressive reduction in the morphological diversity. At ½× MIC, the colonies were predominantly round with mixed white-red pigmentation, whereas at 1× and 2× MIC, the surviving colonies were mainly small, round, flat, dry, red-pigmented, and had predominantly undulated margins (Table 3 and Figure 3).

Colony diameter by specimen source

Colony diameter also differed significantly according to the specimen source (Table 4). Because the four specimen groups were mutually exclusive and of equal size (n=12 each), they permitted a formal comparison. Kruskal-Walli's testing showed significant differences between sources under every condition (M9, p=0.002; RB, p=0.047; ½× MIC, p<0.001; 1× MIC, p=0.010; 2× MIC, p=0.044). Urinary and wound swab isolates produced the largest colonies on antibiotic-free media but were most strongly suppressed by ceftazidime, with median diameters of 0.00 mm at and above the MIC. In contrast, tracheal aspirate isolates, which showed the highest rates of ceftazidime resistance and ESBL production, retained the largest median colony diameter at 1× MIC (6.00 mm) and 2× MIC (5.00 mm) of any source.

Table 1: Characteristics of the representative clinical *P. aeruginosa* isolates.

Specimen source	N	CAZ-resistant, N (%)	ESBL, N (%)	MBL, N (%)	Strong biofilm, N (%)
Pus	12	08 (66.7)	05 (41.7)	03 (25.0)	04 (33.3)
Wound swab	12	08 (66.7)	06 (50.0)	05 (41.7)	10 (83.3)
Urine	12	08 (66.7)	05 (41.7)	03 (25.0)	03 (25.0)
Tracheal aspirate	12	10 (83.3)	07 (58.3)	05 (41.7)	05 (41.7)
Total	48	34 (70.8)	23 (47.9)	16 (33.3)	22 (45.8)

CAZ: ceftazidime; ESBL: extended-spectrum β-lactamase; MBL: metallo-β-lactamase. Values are expressed as N (%) unless otherwise specified

Table 2: Effect of increasing ceftazidime concentrations on colony growth and colony diameter.

Experimental condition	Growth, N (%)	Growing isolates only, mean±SD (mm)	All 48 isolates, mean±SD (mm)	All 48 isolates, median [IQR] (mm)
M9 (control)	46 (95.8)	20.57±16.91	19.71±17.06	10.50 [07.00-33.25]
RB	47 (97.9)	19.59±09.48	19.18±09.79	16.50 [12.00-25.50]
RB + ½× MIC	31 (64.6)	06.13±01.67	03.96±03.25	05.00 [00.00-06.00]
RB + 1× MIC	24 (50.0)	05.83±10.74	02.92±03.19	02.00 [00.00-06.00]
RB + 2× MIC	22 (45.8)	05.00±01.45	02.29±02.70	00.00 [00.00-00.00]

RB, M9 minimal agar supplemented with Congo red and Coomassie brilliant blue; MIC: isolate-specific minimum inhibitory concentration; SD: standard deviation; IQR: interquartile range. The three right-hand columns report the colony diameter in millimetres. Growth was defined as the number of isolates producing visible colonies; the remainder showed no growth. Colony diameter is reported in two ways: among isolates showing visible growth, which isolates the effect on colony size, and across all 48 isolates with non-viable (no-growth) colonies assigned a diameter of 0 mm, which combines the effects of growth inhibition and colony size reduction. Because the same 48 isolates were assessed under all five conditions, differences in the proportion showing visible growth were assessed using Cochran's Q test (Q=75.47, df=4, p<0.001) with pairwise McNemar tests, and differences in colony diameter were assessed using the Friedman test for related samples (χ^2 =149.00, df =4, p<0.001) with Wilcoxon signed-rank post-hoc comparisons and Bonferroni correction. Median values are reported because the all-isolate distribution is zero-inflated at higher ceftazidime concentrations

Table 3: Summary of predominant colony morphology under increasing ceftazidime concentrations.

Characteristic	M9	RB	½× MIC	1× MIC	2× MIC
Growth	Abundant	Abundant	Reduced	Markedly reduced	Minimal
Colony form	Round, irregular, wrinkled	Round, irregular	Predominantly round	Predominantly round	Predominantly round
Colour	White	White-red	White-red	Predominantly red	Predominantly red
Surface	Dry, shiny, mucoid	Predominantly dry	Shiny to dry	Predominantly dry	Predominantly dry
Elevation	Flat	Flat to raised	Flat	Flat	Flat
Margin	Undulate	Irregular	Entire to undulate	Undulate	Undulate

RB, M9 minimal agar supplemented with Congo red and Coomassie brilliant blue; MIC: isolate-specific minimum inhibitory concentration

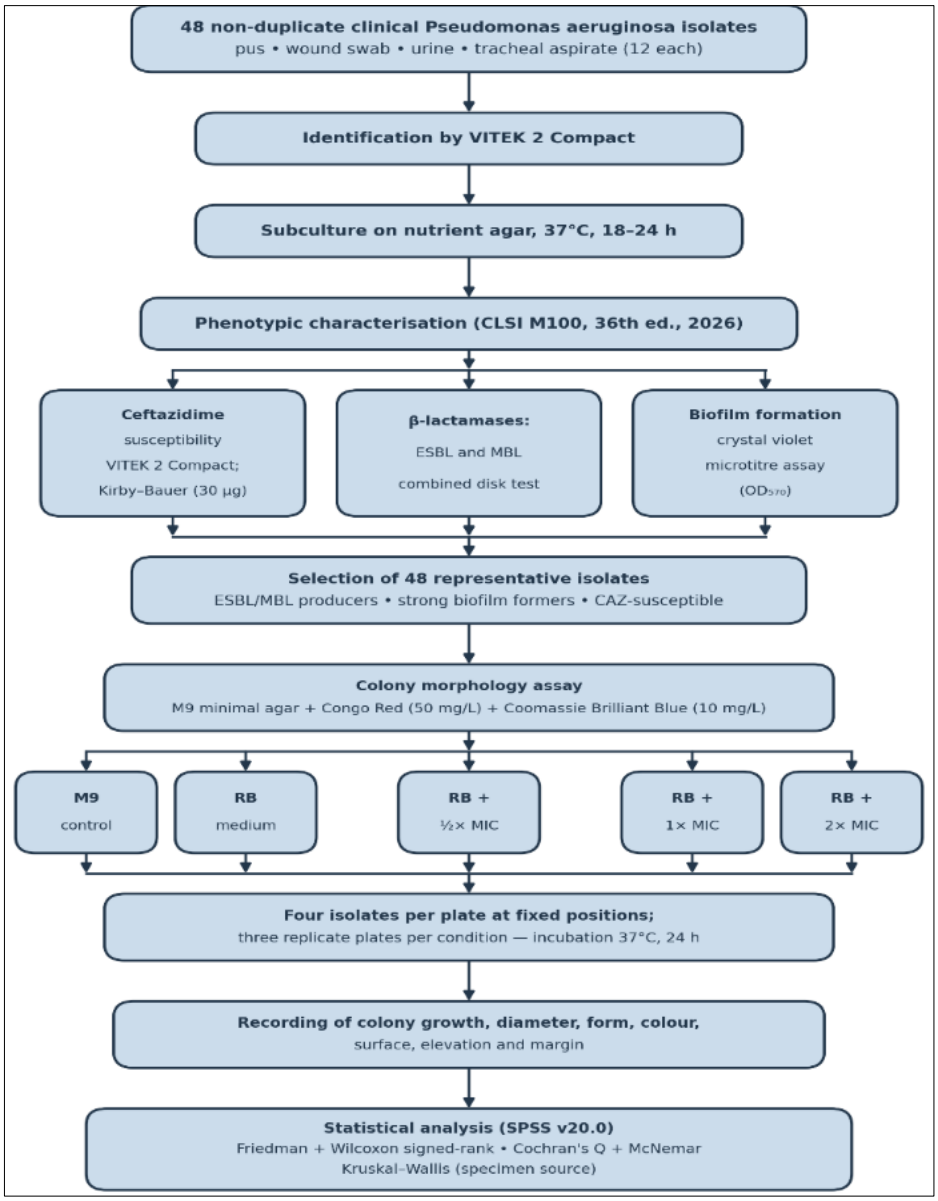


Figure 1: Experimental workflow. Schematic overview of the study, showing the collection and identification of clinical *P. aeruginosa* isolates from pus, wound swabs, urine, and tracheal aspirate specimens; characterisation of ceftazidime susceptibility by VITEK 2 compact, ESBL and MBL production by combined disk testing, and biofilm formation by crystal violet assay; selection of representative isolates; and evaluation of colony morphology on M9 minimal agar supplemented with congo red and coomassie brilliant blue (RB medium) at one-half, one, and two times the isolate-specific minimum inhibitory concentration (MIC) of ceftazidime.

Table 4: Median colony diameter by specimen source under increasing ceftazidime concentrations.

Specimen source	M9	RB	½× MIC	1× MIC	2× MIC
Pus	07.00	10.50	06.00	02.00	00.00
Wound swab	33.00	22.50	02.00	00.00	00.00
Urine	38.00	19.50	00.00	00.00	00.00
Tracheal aspirate	08.00	18.50	04.50	06.00	05.00
P value	00.002	0.047	<0.001	0.010	0.044

Values are the median colony diameter (mm) across all isolates in each group, with non-viable (no growth) colonies assigned a diameter of 0 mm. MIC: isolate-specific minimum inhibitory concentration; RB, M9 minimal agar supplemented with Congo red and Coomassie brilliant blue. The specimen source groups were mutually exclusive and of equal size (n=12); therefore, differences between sources were assessed using the Kruskal-Wallis test

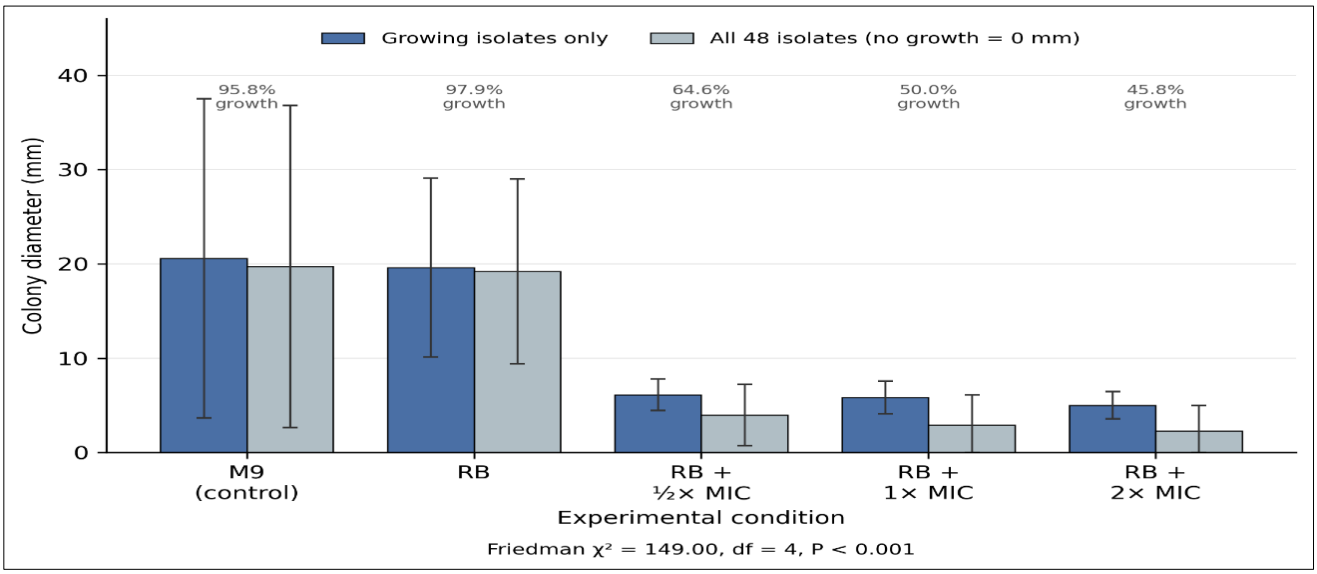


Figure 2: Bar graph showing the mean colony diameter. Mean colony diameter (mm) of clinical *P. aeruginosa* isolates across the five experimental conditions (M9 control, RB, and RB supplemented with ceftazidime at ½×, 1×, and 2× MIC). Paired bars show the mean colony diameter calculated in two ways: among isolates showing visible growth (dark bars) and across all 48 isolates with non-viable colonies assigned a diameter of 0 mm (light bars). Error bars represent one standard deviation truncated at zero because negative diameters are not possible. The percentage of isolates showing visible growth under each condition is indicated above the bars. Colony diameter decreased significantly with increasing ceftazidime concentrations (Friedman test, p<0.001).

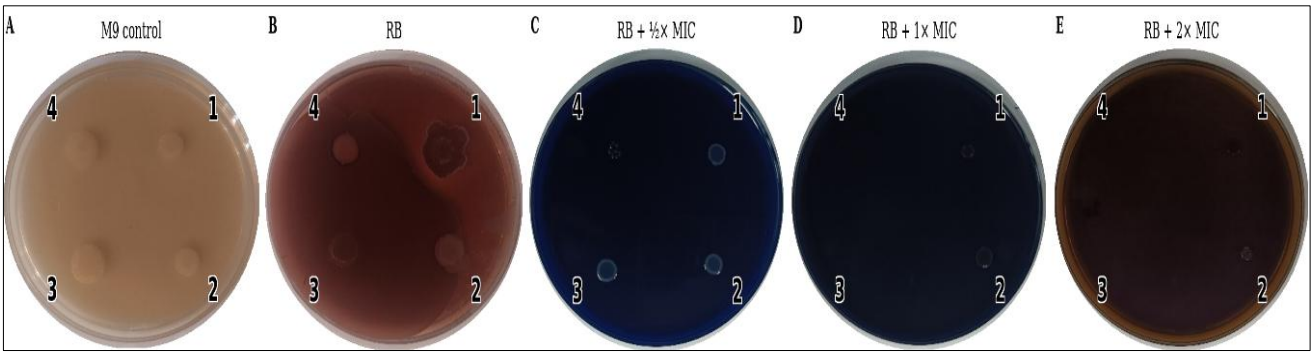


Figure 3: Representative colony photographs are shown. Colony morphology of clinical *P. aeruginosa* isolates grown for 24 hours at 37°C on M9 control agar, RB medium, and RB medium supplemented with ceftazidime at ½×, 1×, and 2× isolate-specific MIC. Increasing ceftazidime concentrations were associated with reduced colony size and a shift from diverse morphologies to predominantly small, round, flat, dry, and red-pigmented colonies with increased ceftazidime concentrations. On each plate, the four isolates occupied fixed positions: 1, ESBL producer; 2, MBL producer; 3, strong biofilm former; and 4, ceftazidime-susceptible isolate.

DISCUSSION

In this study, we found that increasing ceftazidime concentrations altered the growth and colony morphology of clinical *P. aeruginosa* in a dose-dependent manner. Ceftazidime suppressed growth; however, the surviving colonies showed clear phenotypic shifts, namely smaller size and simpler morphology. This indicates that antibiotic stress affects not only the viability but also the phenotype of the surviving population, allowing a subset of isolates to persist under drug pressure.

The stepwise decrease in colony diameter and loss of morphological variety agrees with earlier work showing that β-lactams can change bacterial growth kinetics and physiology, respectively. Such stress has been linked to altered cell wall synthesis, metabolic activity, and matrix production, which in turn reshape colony architecture.[18,21] The shift towards small, round, dry, red-pigmented colonies at higher concentrations points to the selection of phenotypes suited to adverse conditions.[31] Adding Congo red and Coomassie brilliant blue made these changes easier to see and offered a straightforward way to read colony architecture during drug exposure.

The isolates examined here carried β-lactamase determinants and frequently formed biofilms, both of which are established contributors to *P. aeruginosa* persistence in chronic infections. Biofilm-embedded cells are less susceptible to antimicrobials owing to limited drug penetration, slowed metabolism, and the presence of persistent cells. Nearly half of the isolates studied were strong biofilm formers, and the majority carried β-lactamase determinants; therefore, the population surviving ceftazidime exposure was likely to have been enriched for isolates possessing one or both of these traits.[16,32] Although the resistance determinants were defined phenotypically, the molecular basis of the morphological changes themselves was not investigated; the results are nonetheless consistent with stress-induced phenotypic adaptation acting alongside these known mechanisms. Work at the molecular level is needed to define the roles of quorum sensing, exopolysaccharide production, and stress-response pathways in the phenotypes observed.[4]

The differences observed between the specimen sources merit further discussion. Urinary and wound swab isolates grew largest in the absence of antibiotics but were the most completely suppressed by ceftazidime, whereas tracheal aspirate isolates sustained measurable growth at and above the MIC. This pattern parallels the higher rates of ceftazidime resistance, ESBL production, and MBL production among tracheal aspirate isolates and is consistent with the selective pressure exerted by repeated antimicrobial exposure in ventilated patients. The uncoupling of growth capacity in the absence of antibiotics from growth capacity under antibiotic stress suggests that colony size on antibiotic-free medium is a poor proxy for the ability to persist during therapy.

These observations are clinically relevant because ceftazidime is a key treatment option for *P. aeruginosa* infections. The persistence of morphologically altered colonies after drug exposure suggests that the surviving population may exhibit traits favouring continued survival during therapy.[33] Recognising such responses could aid in understanding persistence and inform future studies linking colony morphology, resistance, and treatment outcomes.

This study has several limitations. The experiments used representative clinical isolates under defined in vitro conditions, which cannot reproduce the host environment during infection. Morphology was assessed at a single time point. Resistance determinants were defined phenotypically rather than confirmed at the molecular level, and no transcriptional or regulatory work was performed to tie those determinants to morphological changes; therefore, the mechanistic basis of the changes remains unknown. The analysis has its own constraints. Colony diameter under ceftazidime is zero-inflated: a large share of isolates failed to grow, the all-isolate median was 0 mm at 1× and 2× MIC, and the mean must therefore be read alongside the growth frequencies in Table 2. The diameter was not broken down by resistance phenotype because one isolate may produce ESBL and MBL and form a strong biofilm; these categories overlap too heavily for a formal between-group test at this sample size. Answering this question would require mutually exclusive resistance categories and a larger series. Replicate plates were prepared, but the diameter was recorded once per isolate per condition; therefore, within-isolate measurement variability could not be estimated. The specimen-source differences were based on 12 isolates per group and need confirmation in a larger study. Pairing phenotypic assessment with transcriptomic, proteomic, or genomic methods would give a fuller account of how the organism adapts to antibiotic stress.[34]

Increasing ceftazidime concentrations altered the growth and colony morphology of clinical *P. aeruginosa*. Reading these changes on M9 agar with Congo red and Coomassie brilliant blue reveals a form of adaptation that routine susceptibility testing does not capture. The molecular mechanisms driving these phenotypic shifts and their implications for persistence during therapy remain to be elucidated.

CONCLUSION

Increasing ceftazidime concentrations reduced both the proportion of clinical *P. aeruginosa* isolates able to grow and the size of the colonies formed by those that did, while narrowing colony morphology to a uniform small, round, flat, dry, red-pigmented form. The extent of suppression varied with specimen source, tracheal aspirate isolates being the least affected at and above the MIC. These findings describe the phenotype of the surviving population rather than its susceptibility category alone, and require confirmation in a larger, resistance-stratified series

before any inference about persistence during therapy can be drawn.

ACKNOWLEDGEMENTS

Authors would like to thank the technical staff of the Department of Microbiology, Nazareth Hospital, for their assistance with bacterial identification using the VITEK 2 compact system and for archiving the clinical isolates used in this study.

Funding: No funding sources
Conflict of interest: None declared
Ethical approval: The study was approved by the Institutional Ethics Committee

REFERENCES

1. Reynolds D, Kollef M. The epidemiology and pathogenesis and treatment of Pseudomonas aeruginosa infections: an update. Drugs. 2021;81:2117-31.
2. Wood SJ, Kuzel TM, Shafikhani SH. Pseudomonas aeruginosa: infections, animal modeling, and therapeutics. Cells. 2023;12(1):199.
3. Reynolds D, Burnham JP, Vazquez Guillamet C, McCabe M, Yuenger V, Betthauser K, et al. The threat of multidrug-resistant/extensively drug-resistant Gram-negative respiratory infections: another pandemic. Eur Respir Rev. 2022;31(166):220068.
4. Qin S, Xiao W, Zhou C, Pu Q, Deng X, Lan L, et al. Pseudomonas aeruginosa: pathogenesis, virulence factors, antibiotic resistance, interaction with host, technology advances and emerging therapeutics. Signal Transduct Target Ther. 2022;7(1):199.
5. Jangra V, Sharma N, Chhillar AK. Therapeutic approaches for combating Pseudomonas aeruginosa infections. Microbes Infect. 2022;24(4):104950.
6. Pang Z, Raudonis R, Glick BR, Lin TJ, Cheng Z. Antibiotic resistance in Pseudomonas aeruginosa: mechanisms and alternative therapeutic strategies. Biotechnol Adv. 2019;37(1):177-92.
7. Langendonk RF, Neill DR, Fothergill JL. The building blocks of antimicrobial resistance in Pseudomonas aeruginosa: implications for current resistance-breaking therapies. Front Cell Infect Microbiol. 2021;11:665759.
8. Elfadadny A, Ragab RF, AlHarbi M, Badshah F, Ibáñez-Arancibia E, Farag A, et al. Antimicrobial resistance of Pseudomonas aeruginosa: navigating clinical impacts, current resistance trends, and innovations in breaking therapies. Front Microbiol. 2024;15:1374466.
9. Zhao Y, Chen D, Chen K, Xie Y, Yang H, Chen X, et al. Multidrug resistance in Pseudomonas aeruginosa: genetic control mechanisms and therapeutic advances. Mol Biomed. 2024;5:62.
10. Lorusso AB, Carrara JA, Barroso CDN, Tuon FF, Faoro H. Role of efflux pumps on antimicrobial resistance in Pseudomonas aeruginosa. Int J Mol Sci. 2022;23:15779.
11. Sati H, Carrara E, Savoldi A, Hansen P, Garlasco J, Campagnaro E, et al. The WHO bacterial priority pathogens list 2024: a prioritisation study to guide research, development, and public health strategies against antimicrobial resistance. Lancet Infect Dis. 2025;25:1033-43.
12. Asmare Z, Reta MA, Gashaw Y, Getachew E, Sisay A, Gashaw M, et al. Antimicrobial resistance profile of Pseudomonas aeruginosa clinical isolates from healthcare-associated infections in Ethiopia: a systematic review and meta-analysis. PLoS One. 2024;19:e0308946.
13. Thi MTT, Wibowo D, Rehm BHA. Pseudomonas aeruginosa biofilms. Int J Mol Sci. 2020;21:8671.
14. Ghosh S, Mukherjee S, Sarkar S, Chattopadhyay D, Chakraborty A. Biofilm formation and antibiotic resistance in Pseudomonas aeruginosa. Med Microecol. 2024;20:100107.
15. Thöming JG, Häussler S. Pseudomonas aeruginosa is more tolerant under biofilm than under planktonic growth conditions: a multi-isolate survey. Front Cell Infect Microbiol. 2022;12:851784.
16. Ciofu O, Moser C, Jensen PØ, Høiby N. Tolerance and resistance of microbial biofilms. Nat Rev Microbiol. 2022;20:621-35.
17. Sharma D, Misba L, Khan AU. Antibiotics versus biofilm: an emerging battleground in microbial communities. Antimicrob Resist Infect Control. 2023;12:76.
18. Starkey M, Hickman JH, Ma L, Zhang N, De Long S, Hinz A, et al. Pseudomonas aeruginosa rugose small-colony variants have adaptations that likely promote persistence in the cystic fibrosis lung. J Bacteriol. 2009;191:3492-503.
19. Karygianni L, Ren Z, Koo H, Thurnheer T. Biofilm matrixome: extracellular components in structured microbial communities. Trends Microbiol. 2020;28:668-81.
20. Kirisits MJ, Prost L, Starkey M, Parsek MR. Characterization of colony morphology variants isolated from Pseudomonas aeruginosa biofilms. Appl Environ Microbiol. 2005;71:4809-21.
21. Friedman L, Kolter R. Two genetic loci produce distinct carbohydrate-rich structural components of the Pseudomonas aeruginosa biofilm matrix. J Bacteriol. 2004;186:4457-65.
22. Bisht K, Luecke AR, Wakeman CA. Temperature-specific adaptations and genetic requirements in a biofilm formed by Pseudomonas aeruginosa. Front Microbiol. 2022;13:1032520.
23. Harsh T, Patil HV, Patil SR. Prevalence and antimicrobial susceptibility pattern of Pseudomonas aeruginosa isolates from various clinical specimens in a tertiary care hospital: an analysis of resistance trends and implications for treatment strategies. Cureus. 2024;16:e72564.

24. Cendra MDM, Torrents E. Pseudomonas aeruginosa biofilms and their partners in crime. Biotechnol Adv. 2021;49:107734.
25. Funke G, Monnet D, deBernardis C, von Graevenitz A, Freney J. Evaluation of the VITEK 2 system for rapid identification of medically relevant gram-negative rods. J Clin Microbiol. 1998;36:1948-52.
26. CLSI. Performance standards for antimicrobial susceptibility testing. 36th ed. CLSI supplement M100. Wayne, PA: Clinical and Laboratory Standards Institute; 2026.
27. Bauer AW, Kirby WM, Sherris JC, Turck M. Antibiotic susceptibility testing by a standardized single disk method. Am J Clin Pathol. 1966;45:493-6.
28. Sasirekha B, Manasa R, Ramya P, Sneha R. Frequency and antimicrobial sensitivity pattern of extended spectrum beta-lactamases producing Escherichia coli and Klebsiella pneumoniae isolated in a tertiary care hospital. Al Ameen J Med Sci. 2010;3:265-71.
29. Yong D, Lee K, Yum JH, Shin HB, Rossolini GM, Chong Y. Imipenem-EDTA disk method for differentiation of metallo-beta-lactamase-producing clinical isolates of Pseudomonas spp. and Acinetobacter spp. J Clin Microbiol. 2002;40:3798-801.
30. Stepanović S, Vuković D, Hola V, Di Bonaventura G, Djukić S, Ćirković I, et al. Quantification of biofilm in microtiter plates: overview of testing conditions and practical recommendations for assessment of biofilm production by staphylococci. APMIS. 2007;115:891-9.
31. Ha DG, O'Toole GA. c-di-GMP and its effects on biofilm formation and dispersion: a Pseudomonas aeruginosa review. Microbiol Spectr. 2015;3:MB-0003-2014.
32. Ciofu O, Rojo-Molinero E, Macià MD, Oliver A. Antibiotic treatment of biofilm infections. APMIS. 2022;130(143):S1-51.
33. Camus L, Vandenesch F, Moreau K. From genotype to phenotype: adaptations of Pseudomonas aeruginosa to the cystic fibrosis environment. Microb Genom. 2021;7(3):mgen000513.
34. Rossi E, La Rosa R, Bartell JA, Marvig RL, Haagensen JAJ, Sommer LM, et al. Pseudomonas aeruginosa adaptation and evolution in patients with cystic fibrosis. Nat Rev Microbiol. 2021;19(5):331-42.

Cite this article as: Rymbai M, Borah VV. Phenotypic adaptation of clinical *Pseudomonas aeruginosa* to increasing ceftazidime exposure. Int J Basic Clin Pharmacol 2026;15:1144-52.